Appl. Phys. B 80, 291–294 (2005)
DOI: 10.1007/s00340-004-1711-3

Applied Physics B
Lasers and Optics

C. CHENG✉
X. WANG
Z. FANG
B. SHEN

Nonlinear copropagation of two optical pulses of different frequencies in photonic crystal fibers

Laboratory for High Intensity Optics, Shanghai Institute of Optics and Fine Mechanics, Chinese Academy of Sciences, Shanghai 201800, P.R. China

Received: 3 September 2004 /
Revised version: 1 November 2004
Published online: 18 January 2005 •

ABSTRACT A theoretical investigation of the nonlinear copropagation of two optical pulses of different frequencies in a photonic crystal fiber is presented. Different phenomena are observed depending on whether the wavelength of the signal pulse is located in the normal or the anomalous dispersion region. In particular, it is found that the phenomenon of pulse trapping occurs when the signal wavelength is located in the normal dispersion region while the pump wavelength is located in the anomalous dispersion region. The signal pulse suffers cross-phase modulation by the Raman shifted soliton pulse and it is trapped and copropagates with the Raman soliton pulse along the fiber. As the input peak power of the pump pulse is increased, the red-shift of the Raman soliton is considerably enhanced with the simultaneous further blue-shift of the trapped pulse to satisfy the condition of group velocity matching.

PACS 42.65.Tg; 42.81.Dp

1 Introduction

Photonic crystal fibers (PCFs) [1, 2] have recently attracted significant attention because of their specifically controlled dispersion properties and their great potential applications in the fields of optical frequency metrology, sensor technology, and optical telecommunication [3–5]. These fibers commonly consist of a fused-silica core surrounded by an ordered array of microscopic air holes running along its length. The air holes form a low-index cladding around the solid silica core. Therefore, light is guided by total internal reflection as in standard step-index fibers. But, the large difference of refractive index between the 1–3 μm diameter core and the holey cladding provides a very strong specifically controlled waveguide contribution to the dispersion. Therefore, the optical properties of a PCF differ remarkably from those of standard fibers, including 'endlessly sing-mode' behavior [6], novel group velocity dispersion characteristics such as zero-dispersion wavelength shifting to the near infrared [7], and enhanced effective nonlinearity due to the reduced mode size in the core [8]. This combination of the unique dispersion properties and enhanced nonlinearities has made PCFs a promising medium for nonlinear interaction studies and there have been numerous experimental and theoretical investigations of the nonlinear propagation of a single pulse near the zero group-velocity dispersion point of this fiber [9–13]. A few experimental studies of the efficient anti-Stokes signal generation by using two colored pulses in PCFs have also recently been reported [14, 15]. However, to the best of our knowledge, the nonlinear copropagation of two optical pulses of different frequencies in PCFs has not yet been theoretically investigated in detail.

In this paper, a theoretical investigation of the nonlinear copropagation of two optical pulses of different frequencies in a PCF is presented. Different phenomena are observed depending on whether the wavelength of the signal pulse is located in the normal or the anomalous dispersion region. In particular, it is found that the phenomenon of pulse trapping occurs when the signal wavelength is located in the normal dispersion region while the pump wavelength is located in the anomalous dispersion region. The signal pulse suffers cross-phase modulation (XPM) by the Raman shifted soliton pulse and it is trapped and copropagates with the Raman soliton pulse along the fiber. As the input power of the pump pulse is increased, the red-shift of the Raman soliton is considerably enhanced with the simultaneous further blue-shift of the trapped pulse to satisfy the condition of group velocity matching. These XPM-induced frequency shifts may be useful for wavelength conversion of signals in optical communication systems.

2 Numerical model

To understand the nonlinear copropagation of two optical pulses of different frequencies in a PCF, we have numerically solved the strict coupled nonlinear Schrödinger equations using a standard split-step Fourier algorithm [16]:

$$\frac{\partial A}{\partial z}+\sum_{n=2}\beta_{nA}\frac{\mathrm{i}^{n-1}}{n!}\frac{\partial^n}{\partial T^n}A = \mathrm{i}\gamma_A\left(|A|^2A+2|B|^2A+\frac{\mathrm{i}}{\omega_{0A}}\frac{\partial|A|^2A}{\partial T}-T_\mathrm{R}A\frac{\partial|A|^2}{\partial T}\right), \quad (1)$$

✉ Fax: +86-021-6991-8800, E-mail: ccfu@mail.siom.ac.cn

$$\frac{\partial B}{\partial z} - d\frac{\partial B}{\partial T} + \sum_{n=2} \beta_{nB} \frac{\mathrm{i}^{n-1}}{n!} \frac{\partial^n}{\partial T^n} B$$
$$= \mathrm{i}\gamma_B \left(|B|^2 B + 2|A|^2 B + \frac{\mathrm{i}}{\omega_{0B}} \frac{\partial |B|^2 B}{\partial T} - T_\mathrm{R} B \frac{\partial |B|^2}{\partial T} \right), \quad (2)$$

where A and B represent the amplitudes of the pulse envelopes for the pump pulse and the signal pulse, respectively. z is the longitudinal coordinate along the fiber. $T = t - \beta_{1A} z$ is the time in a reference frame traveling with the pump light, where t is the time and β_{1A} is the first-order dispersion for the pump pulse. β_n is the nth-order dispersion coefficient at the central frequency ω_0. $\gamma = n_2\omega_0/cA_\mathrm{eff}$ is the nonlinear coefficient, $n_2 \approx 3.0 \times 10^{-20}\,\mathrm{m}^2/\mathrm{W}$ is the nonlinear refractive index of fused-silica glass, and A_eff is the effective mode area of the fiber. ω_{0A} and ω_{0B} are the center angular frequencies for the pump and the signal pulses. $T_\mathrm{R} = 5\,\mathrm{fs}$ is the coefficient for the Raman scattering. The parameter d is a measure of group-velocity mismatch between the two colored pulses. The left-hand sides of the above equations represent the linear effects; the effects of the chromatic dispersion are included. The right-hand sides correspond to the nonlinear effects; self-phase modulation (SPM), XPM, self-steepening (SST), and intrapulse stimulated Raman scattering (ISRS) are considered.

We consider a PCF with a core size of 2 μm in diameter used in [12]. The zero-dispersion wavelength of the fiber is 767 nm. At a wavelength of 800 nm, the nonlinear coefficient is estimated to be $\gamma = 0.075\,(\mathrm{W\,m})^{-1}$, and the dispersion coefficients up to sixth order are $\beta_2 = -5.9998 \times 10^{-6}\,\mathrm{fs}^2/\mathrm{nm}$, $\beta_3 = 6.0445 \times 10^{-5}\,\mathrm{fs}^3/\mathrm{nm}$, $\beta_4 = -3.3683 \times 10^{-5}\,\mathrm{fs}^4/\mathrm{nm}$, $\beta_5 = -4.7893 \times 10^{-5}\,\mathrm{fs}^5/\mathrm{nm}$, $\beta_6 = 3.3037 \times 10^{-4}\,\mathrm{fs}^6/\mathrm{nm}$. At a wavelength of 740 nm, the nonlinear coefficient is estimated to be $\gamma = 0.081\,(\mathrm{W\,m})^{-1}$, and the dispersion coefficients up to sixth order are $\beta_2 = 4.9731 \times 10^{-6}\,\mathrm{fs}^2/\mathrm{nm}$, $\beta_3 = 5.4568 \times 10^{-5}\,\mathrm{fs}^3/\mathrm{nm}$, $\beta_4 = -2.9155 \times 10^{-5}\,\mathrm{fs}^4/\mathrm{nm}$, $\beta_5 = 6.3452 \times 10^{-6}\,\mathrm{fs}^5/\mathrm{nm}$, $\beta_6 = -1.1828 \times 10^{-4}\,\mathrm{fs}^6/\mathrm{nm}$. $d = 1/v_{gA} - 1/v_{gB} = 1.24 \times 10^{-6}\,\mathrm{fs/nm}$ for the pump wavelength is 800 nm and for the signal wavelength is 740 nm. The fiber loss is neglected since only a short length of the fiber is considered in the simulations.

The input pulses are assumed to have the forms

$$A(z=0, T) = \sqrt{P_1}\,\mathrm{sech}(T/T_1)\,, \quad (3)$$
$$B(z=0, T) = \sqrt{P_2}\,\mathrm{sech}((T - T_\mathrm{d})/T_2)\,, \quad (4)$$

where $P_1 = A_0^2$ and $P_2 = B_0^2$ are the input peak powers of the pump pulse and the signal pulse, respectively. For the pump pulse and the signal pulse, 100 fs (i.e. $T_1 = 100\,\mathrm{fs}$) and 200 fs (i.e. $T_2 = 200\,\mathrm{fs}$) transform-limited sech^2 pulses are assumed, where T_1 and T_2 are related to the initial full width at half maximum (FWHM) by $T_\mathrm{FWHM1,2} \approx 1.763 T_{1,2}$. We assume that the center of the signal pulse is delayed from that of the pump pulse temporally by 40 fs (i.e. $T_\mathrm{d} = 40\,\mathrm{fs}$) because the pump pulse is slower than the signal pulse (see Fig. 2b (A)). The pump pulse is coupled into the fiber slightly before the signal pulse and then a collision occurs between the pump pulse and the signal pulse during the pulse propagation.

3 Numerical results

Figure 1 shows the characteristics of the output spectra of the two optical pulses of different frequencies for varying the wavelength of the pump pulse (red line) and the signal pulse (black line) when the power of the pump pulse is 200 W and the power of the signal pulse is 1 W. When both the wavelengths of the pump pulse and the signal pulse are located in the normal dispersion region, as seen in Fig. 1a, the temporal and spectral behavior of the pump pulse typical for SPM is found and the signal pulse splits into two spectrum peaks due to the effect of the XPM by the pump pulse. When both the wavelengths of the pump pulse and the signal pulse are located in the anomalous dispersion region, as seen in Fig. 1c, soliton-fission mechanisms [17] play an important role for the pump-pulse propagation and the spectrum of the signal pulse is slightly broadened due to the effect of the XPM by the pump pulse. The behaviors of the pump pulse of the above two cases are in agreement with the trend discussed in [9–11, 13] and the effect of the XPM by the pump pulse on the behavior of the signal pulse is very weak, so that we limit ourselves to a short comment. However, when the pump wavelength is located in the anomalous dispersion region while the wavelength of the signal pulse is located in the normal dispersion region, as seen in Fig. 1b, the effect of the XPM by the soliton pulse on the behavior of the signal pulse becomes very strong; in this case we have observed that the signal pulse is trapped by the Raman shifted soliton pulse and the two pulses copropagate along the fiber, which is very similar to the phenomenon of pulse trapping generated in a conventional optical fiber [16, 18, 19]. When the wavelength of the signal pulse is tuned away from the zero-dispersion wavelength of the PCFs further into the

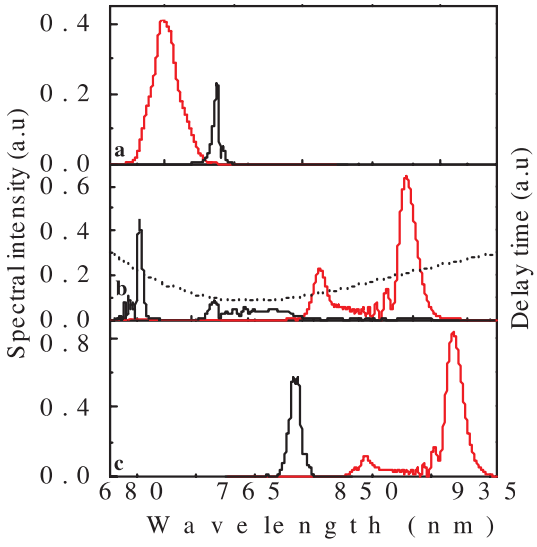

FIGURE 1 The output spectra of the two optical pulses of different frequencies for varying the wavelengths of the pump pulse (*red line*) and the signal pulse (*black line*). **a** $\mathrm{wave}_\mathrm{signal} = 740\,\mathrm{nm}$, $\mathrm{wave}_\mathrm{pump} = 700\,\mathrm{nm}$. **b** $\mathrm{wave}_\mathrm{signal} = 740\,\mathrm{nm}$, $\mathrm{wave}_\mathrm{pump} = 800\,\mathrm{nm}$. **c** $\mathrm{wave}_\mathrm{signal} = 800\,\mathrm{nm}$, $\mathrm{wave}_\mathrm{pump} = 840\,\mathrm{nm}$. The fiber length $L = 96\,\mathrm{cm}$; the input peak powers of the pump pulse and the signal pulse are $P_1 = 200\,\mathrm{W}$ and $P_2 = 1\,\mathrm{W}$, respectively. In order to clarify the behavior of the signal pulse, its spectral intensity is enlarged. The *dotted line* represents the delay time in the fiber owing to chromatic dispersion

normal dispersion region while keeping other conditions the same as in the case of Fig. 1b, the pulse trapping also occurs but the frequency shift is decreased. This difference is clearly related to the influence of walk-off due to the difference in group velocities between the signal pulse and the pump pulse. As shown in Fig. 1b, when pulse trapping occurs, most of the spectral component of the signal pulse is shifted to 682 nm. At this wavelength, the group velocity of the trapped pulse is almost the same as that of the Raman shifted soliton pulse, and the condition of group-velocity matching is satisfied.

To better understand the trapped-pulse generation in a PCF, we have simulated the nonlinear copropagation of the two optical pulses of different frequencies in the case of Fig. 1b. The results are shown in Fig. 2. The pump pulse is initially compressed due to the combined effects of nonlinearities and anomalous dispersion before it breaks into multiple solitons. The compressed pump pulse interacts with the leading edge of the signal pulse (see Fig. 2b (B)) and thus suppress the broadening of the right-hand side of the spectrum of the signal pulse (see Fig. 2a (B)). Subsequently, a Raman soliton is formed and its group velocity is monotonically decreased due to the soliton self-frequency shift (SSFS) [20]; then the delayed Raman soliton pulse interacts with the trailing edge of the signal pulse, which makes the signal pulse see a higher-index wall induced by the Raman shifted soliton pulse and it cannot go ahead of the Raman soliton pulse (see Fig. 2b (C), (D), and (E)). In other words, the signal pulse suffers XPM by the Raman shifted soliton pulse and it is trapped and copropagates with the Raman soliton pulse along the fiber, while the leading part of the signal pulse is not trapped by the Raman soliton pulse and propagates independently. That is to say, the physical mechanism of the pulse trapping is the sequential XPM by the Raman shifted soliton pulse. This phenomenon is not observed when the effect of Raman scattering is not active. The leading part of the trapped pulse is almost always overlapped with the trailing edge of the Raman soliton pulse and the temporal behavior of the trapped pulse is complex. First, the trapped pulse is always caught at the trailing edge of the Raman shifted soliton pulse and can not go ahead of it when the pulse trapping occurs (see Fig. 2b (C, D, E)). Second, the temporal width of the trapped pulse is broadened from about 51-fs to about 190-fs when the propagagion length of the trapped pulse increases from 48 cm to 96 cm. However, if the trapping does not occur, the temporal width of the signal pulse is broadened to be about 265-fs due to the effect of the normal dispersion when the fiber length is 96 cm. That is to say, the signal pulse broadening is suppressed by the pulse trapping. In the corresponding frequency domain, the Raman soliton pulse is continously red-shifted due to the SSFS while the blue shift of the trapped pulse is almost saturated (see Fig. 2a (C), (D) and (E)). This can be explained as follows. As the Raman soliton experiences the SSFS, its width increases due to a change in the dispersion and its peak power decreases. This in turn reduces the efficiency of the blue-shift induced by XPM. We also note that the Raman soliton interact with the signal pulse through XPM, which leads to energy transfer from the red side of the signal pulse to the blue side (see Fig. 2a (C), (D) and (E)). In other words, the amplitude of trapped pulse increases with the propagation length due to the above described energy transfer.

Figure 3 shows the characteristics of wavelength shift of the soliton and the trapped pulse at the output of 96 cm long PCF as the input peak power of the pump pulse is increased while keeping the input peak power of the signal pulse con-

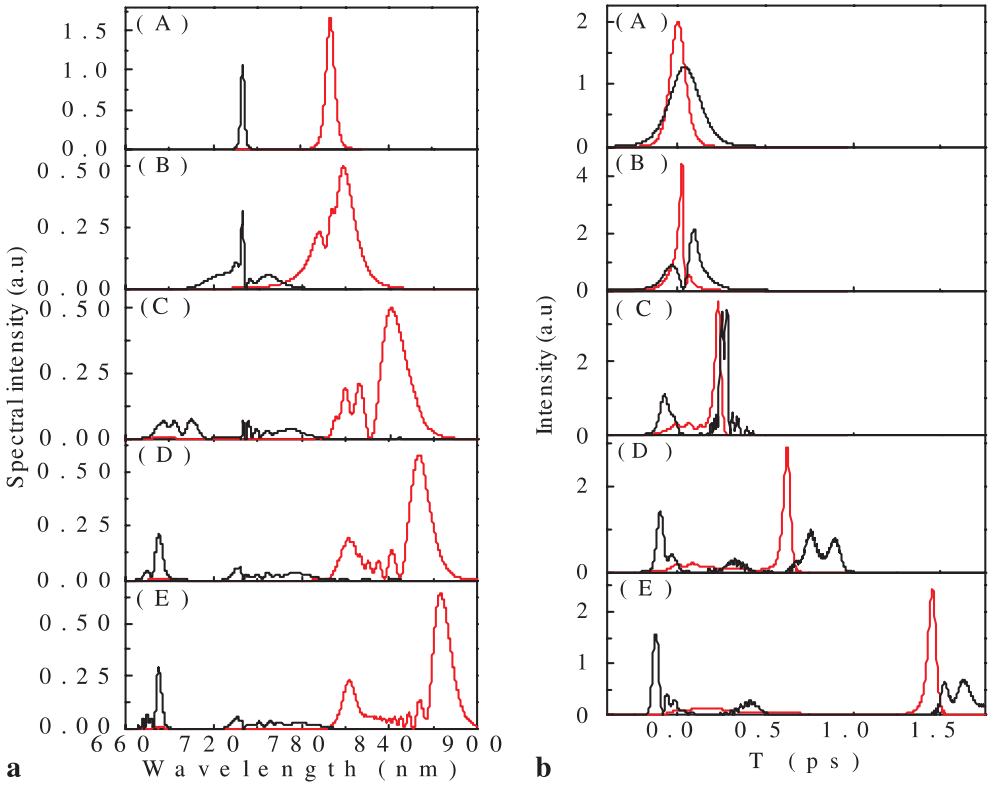

FIGURE 2 The spectral (**a**) and the temporal (**b**) evolutions of the two optical pulses of different frequencies along the fiber. (A) 0 cm, (B) 24 cm, (C) 48 cm, (D) 72 cm, (E) 96 cm. The input powers are $P_1 = 200$ W and $P_2 = 1$ W

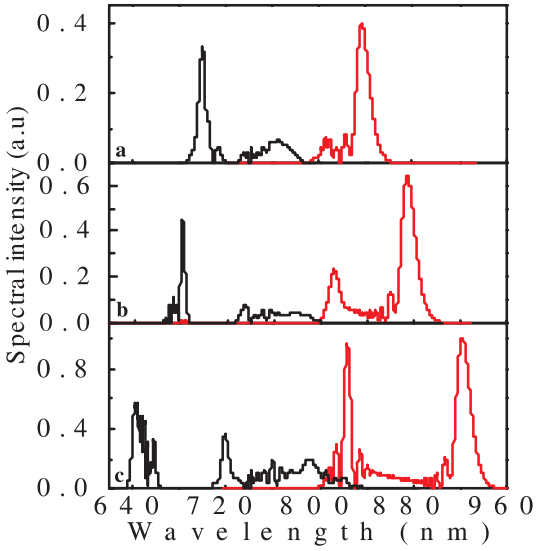

FIGURE 3 The wavelength shift of the output pulses for increasing input peak power of the pump pulse. **a** $P_1 = 100$ W, **b** $P_1 = 200$ W, **c** $P_1 = 400$ W. The fiber length $L = 96$ cm; the input peak power of the signal pulse is $P_2 = 1$ W

stant. As the input peak power of the pump pulse is increased, the red-shift of the Raman soliton is considerably enhanced with the simultaneous further blue-shift if the trapped pulse to satisfy the condition of group velocity matching. As seen in Fig. 3c, when the input peak power of the pump pulse is increased ip to 400 W, the wavelength of the soliton pulse is shifted from 800 to 923 nm and that of the trapped pulse is shifted from 740 to 642 nm. As the input peak power of the pump pulse is increased, the power of the Raman soliton is also increased. The increasing power of the Raman soliton enhances the efficiency of XPM and thus enhancing the blue-shift of the trapped pulse. Therefore, one can obtain much larger wavelength shift of the trapped signal pulse by increasing the input peak power of the pump pulse. We believe that such a blue shift induced by the pulse trapping by the Raman shifted soliton pulse can explain the behavior of the blue shift of both the shorter wavelength side of the supercontinuum and the strong dispersive wave generation in more than several centimeter long PCFs [10, 14, 21–23].

4 Conclusions

As a conclusion, we have presented numerical results describing the nonlinear copropagation of two optical pulses of different frequencies in a PCF. By numerically solving the strict coupled nonlinear Schrödinger equations under different conditions, we were able to follow in detail the evolutions of the two optical pulses of different frequencies as they propagate along the fiber. Different phenomena are observed depending on whether the signal wavelength is located in the normal or the anomalous dispersion region. In particular, it is found that the phenomenon of pulse trapping occurs when the wavelength of the signal pulse is located in the normal dispersion region while the wavelength of the pump pulse is located in the anomalous dispersion region. The signal pulse in the normal dispersion region suffers XPM by the Raman shifted soliton pulse in the anomalous dispersion region and it is trapped and copropagates with the Raman soliton pulse along the fiber. As the input peak power of the pump pulse is increased, the red-shift of the Raman soliton is considerably enhanced with the simultaneous further blue-shift of the trapped pulse to satisfy the condition of group velocity matching. We believe that the blue shift of both the shorter-wavelength components of the supercontinuum and the anti-Stokes pulses in PCFs is induced through the pulse trapping.

ACKNOWLEDGEMENTS This research is supported by the 'Hundred-Talent Project' and the 'Knowledge Innovation' Foundation of the Chinese Academy of Sciences.

REFERENCES

1 J.C. Knight, T.A. Birks, P.S.J. Russell, D.M. Atkin: Opt. Lett. **21**, 1547 (1996)
2 P.S.J. Russell: Science **299**, 358 (2003)
3 T. Udem, R. Holzwarth: Nature **416**, 233 (2002)
4 H. Takara, T. Ohara, K. Mori, K.I. Sato: Electron. Lett. **36**, 2089 (2000)
5 T.M. Monro, W. Belardi, K. Furusawa, J.C. Baggett, N.G. Broderick, D.J. Richardon: Meas. Sci. Technol. **12**, 854 (2001)
6 T.A. Birks, J.C. Knight, P.S.J. Russell: Opt. Lett. **22**, 961 (1997)
7 J.K. Ranka, R.S. Windeler, A.J. Stentz: Opt. Lett. **25**, 25 (2000)
8 N.G.R. Broderick, T.M. Monro, P.J. Bennet, D.J. Richardon: Opt. Lett. **24**, 1395 (1999)
9 A.L. Gaeta: Opt. Lett. **27**, 924 (2002)
10 B.R. Washburn, S.E. Ralph, R.S. Windeler: Opt. Express **10**, 575 (2002)
11 G. Genty, M. Lehtonen, H. Ludvigsen, J. Broeng, M. Kaivola: Opt. Express **10**, 1083 (2002)
12 C.F. Cheng, X.F. Wang, B. Lu: Acta Phys. Sin. **53**, 1826 (2004)
13 A.V. Husakou, J. Herrmann: J. Opt. Soc. Am. B **19**, 2171 (2002)
14 S.O. Konorov, A.A. Ivanov, D.A. Akimov, M.V. Alfimov, A.A. Podshivalov, Y.N. Kondrat'ev, V.S. Shevandin, K.V. Dukel'skii, A.V. Khokhlov, A.M. Zheltikov: Laser Phys. **14**, 791 (2004)
15 A.B. Fedotov, S.O. Konorov, V.P. Mitrokhin, E.E. Serebryannikov, A.M. Zheltikov: Phys. Rev. A **70**, 045 802 (2004)
16 G.P. Agrawal: *Nonlinear Fiber Optics* (Academic, New York 2001)
17 A.V. Husakou, J. Herrmann: Phys. Rev. Lett. **87**, 203 901 (2001)
18 M. Shalaby, A. Barthelemy: Opt. Lett. **16**, 1472 (1991)
19 N. Nishizawa, T. Goto: Opt. Express **10**, 1151 (2002)
20 F.M. Mitschke, L.F. Mollenauer: Opt. Lett. **11**, 659 (1986)
21 C.F. Cheng, X.F. Wang, B.F. Shen: Chin. Phys. Lett. **21**, 1965 (2004)
22 I. Cristiani, R. Tediosi, L. Tartara, V. Degiorgio: Opt. Express **12**, 124 (2004)
23 A.B. Fedotov, I. Bugar, E.E. Serebryannikov, D. Chorvatjr, A.M. Zheltikov: Appl. Phys. B **77**, 313 (2003)